Chapter 19

Assessment, Validation, and Refinement of the Atmospheric Correction Algorithm for the Ocean Color Sensors

Menghua Wang
University of Maryland, Baltimore County, Baltimore, Maryland

19.1 INTRODUCTION

The primary focus of this proposed research is for the *atmospheric correction algorithm evaluation and development* and *satellite sensor calibration and characterization*. It is well known that the atmospheric correction, which removes more than 90% of sensor-measured signals contributed from atmosphere in the visible, is the key procedure in the ocean color remote sensing (Gordon and Wang, 1994). The accuracy and effectiveness of the atmospheric correction directly affect the remotely retrieved ocean bio-optical products. On the other hand, for ocean color remote sensing, in order to obtain the required accuracy in the derived water-leaving signals from satellite measurements, an on-orbit vicarious calibration of the whole system, i.e., sensor and algorithms, is necessary. In addition, it is important to address issues of (i) cross-calibration of two or more sensors and (ii) in-orbit vicarious calibration of the sensor-atmosphere system. The goal of these researches is to develop methods for meaningful comparison and possible merging of data products from multiple ocean color missions. In the past year, much efforts have been on (a) understanding and correcting the artifacts appeared in the SeaWiFS-derived ocean and atmospheric produces; (b) developing an efficient method in generating the SeaWiFS aerosol lookup tables, (c) evaluating the effects of calibration error in the near-infrared (NIR) band to the atmospheric correction of the ocean color remote sensors, (d) comparing the aerosol correction algorithm using the single-scattering epsilon (the current SeaWiFS algorithm) vs. the multiple-scattering epsilon method, and (e) continuing on activities for the International Ocean-Color Coordinating Group (IOCCG) atmospheric correction working group. In this report, I will briefly present and discuss these and some other research activities.

19.2. RESEARCH ACTIVITIES AND RESULTS

Earth Curvature Effects Measured by SeaWiFS

This work has been described in an article by Wang (2003). It is a common fact that the Earth's atmosphere is a spherical-shell atmosphere (SSA) rather than a plane-parallel atmosphere (PPA). Thus, the light scattered by the Earth's atmosphere is governed by physics of the radiative transfer equation (RTE) with proper boundary conditions in the SSA system. In the satellite and aircraft remote sensing, however, the PPA model is usually assumed to compute the lookup tables and convert the sensor-measured signals to the desired physical and optical quantities. The PPA assumption is a simple yet very good approximation for solar and sensor zenith angles $< \sim 80°$. Note that the solar and sensor zenith angles in here are defined as a measure at the local surface. In the PPA assumption, however, the solar zenith angles $\geq 90°$ is not defined. When the solar zenith angles $\geq 90°$ in the PPA system, i.e., when the sun is below the horizon, there will be no light scattered out to the top of the atmosphere (TOA) or at the bottom of the surface. We would experience completely darkness in this situation. The ocean color satellite sensor Sea-viewing Wide Field-of-view Sensor (SeaWiFS) acquired imageries with the solar zenith angles $\geq 90°$ and provided good examples of the Earth's curvature effects on the light scattering processing in the SSA system.

On June 26, 2000, SeaWiFS has acquired imageries with significantly extended coverage, adding about another 5 minutes to the normal 40 minutes recording duty cycle. This was a test for the SeaWiFS coverage capability and to find a proper additional coverage for the SeaWiFS routine operation. For the test purpose, the SeaWiFS coverage for that specific orbit was extended significantly. A specific SeaWiFS measurement line, in which the solar zenith angles varies from ~76° to ~94°, was extracted for study and compared with both the PPA and SSA model computations (Wang, 2003). These are briefly described in here.

To understand and interpolate the SeaWiFS measurements, I have carried out the various radiative transfer simulations for the SSA model using the backward Monte-Carlo method that was developed by *Ding and Gordon* (Ding and Gordon, 1994). Figure 19.1 shows simulated results in comparing with the SeaWiFS measurements at wavelengths 443 and 670 nm for atmosphere composed of the molecules (Rayleigh scattering), molecules and aerosols, and molecules and water-clouds. In Fig. 1, the SSA simulations were carried out for the sensor located at the altitude of 705 km (SeaWiFS orbit) with the various SSA atmospheres. Detailed descriptions of the solar-sensor geometry in the SSA model can be found in *Ding and Gordon* (Ding and Gordon, 1994). For each Monte-Carlo simulation, ten million photons were used.

Figs. 19.1(a) and 19.1(b) are comparison results for atmosphere composed of molecules (Rayleigh scattering) with various physical thickness of the atmospheric layer (from 10 km to 100 km). Results from the plane-parallel atmosphere (indicated as "ppa") are also provided for comparisons. Clearly, PPA model makes significant errors (under-estimation) for the solar zenith angles > ~85°. Figs. 1(c) and 1(d) show comparison results for a two-layer SSA model with aerosols located at the bottom 2-km layer (mixed with 22% of molecules). The *Shettle and Fenn* (Shettle and Fenn, 1979) maritime aerosol model with relative humidity of 80% (M80) and aerosol optical thickness at 865 nm $\tau_a(865)$ of 0.1 were used in simulations. Figs. 19.1(e) and 19.1(f) give comparison results for a two-layer SSA model with water-clouds located at the bottom 2-km layer (mixed with 22% of molecules). These are simulations for the cloud optical thickness τ_c of 8 and an effective particle radius r_e of 8 μm with the various physical thicknesses of the SSA layer, e.g., symbol "20, 2 km" is results for a two-layer SSA atmosphere with total physical thickness of 20-km and 2-km layer at the bottom. Signals contributed from ocean waters are ignored in all these simulations. They are negligible in these cases.

As shown in Fig. 19.2, the TOA radiances at the first part (solar zenith angles from ~76° to ~85°) can be best simulated with cloud optical thickness ~8, while the next part can be well approximated with the M80 model for aerosol optical thickness of 0.1. These are comparisons in qualitatively. It is interesting to note that, however, for the very large solar zenith angles (> ~85°), the TOA radiance is very sensitive to the physical thickness of the atmospheric layer assumed in the simulation. Indeed, for the very large solar zenith angles, the TOA radiance is much more sensitive to the change of physical thickness of the layer than to the optical properties of the medium (e.g., compare results of Figs. 19.1(c) and 19.1(e)). This is because, for the SSA model with the large solar zenith angles, photons that are exiting to the TOA through scattering process are limited by the solar-sensor geometry and physical thickness of the layer. The thicker the layer is, the larger the probability that photons can be scattered into the sensor viewing direction, thereby the larger the sensor-measured radiance. At the wavelength 443 nm, the effective thickness of the SSA layer is best approximated by ~40 km, while at the band 670 nm the SSA layer can be approximated by ~20 km. The Rayleigh optical thicknesses for the wavelength at 443 nm and 670 nm are ~0.234 and ~0.045, respectively. This explains different effective physical thicknesses for the wavelengths 443 and 670 nm at which photons can interact with molecules and particles in the radiative transfer process. Photon at the wavelength 443 nm "sees" thicker of the layer than photon at 670 nm because the Rayleigh optical thickness at 443 nm is significantly larger than that of 670 nm. For the PPA model, on the other hand, the physical thickness has no effects on the TOA radiance.

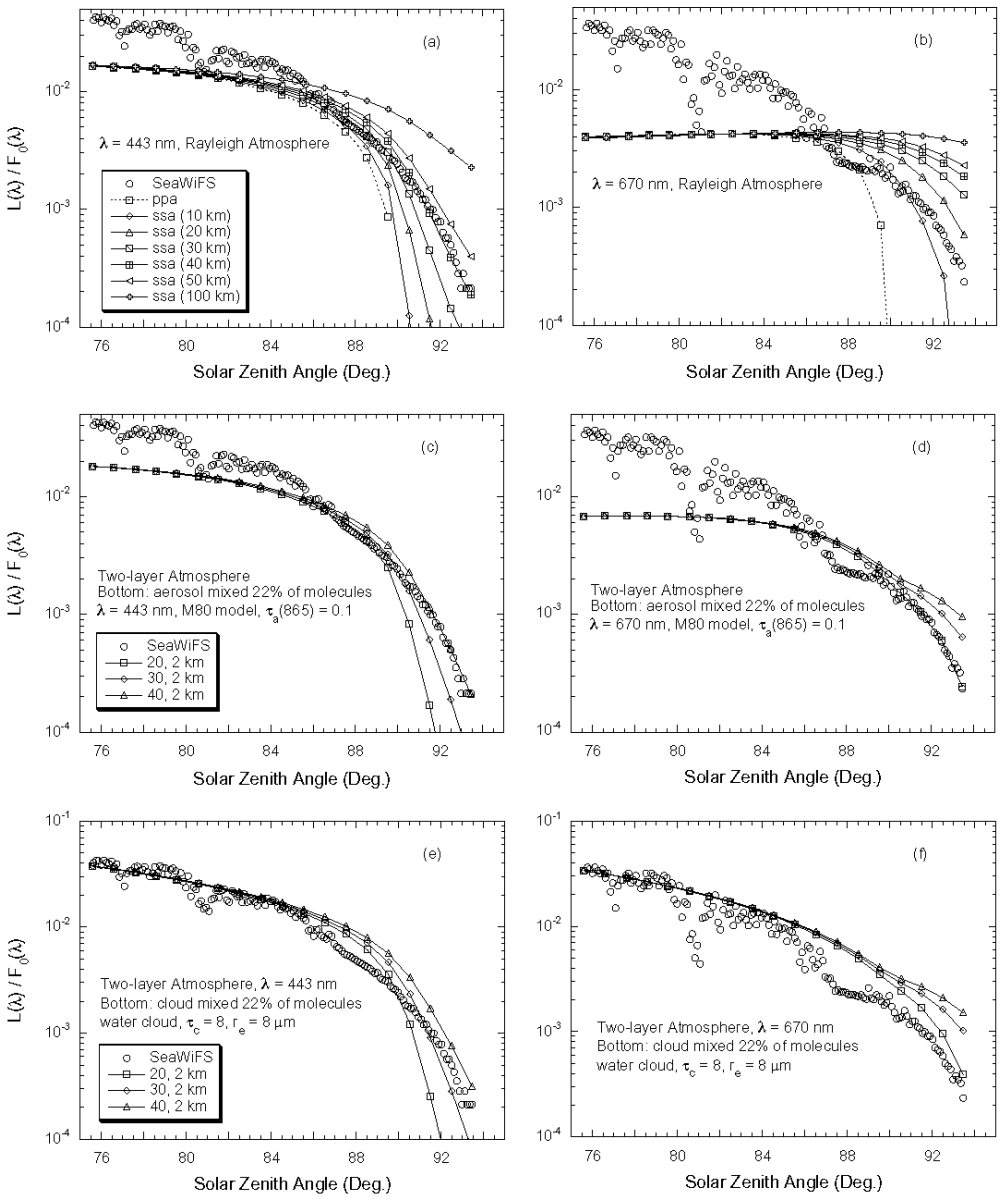

Figure 19.1: The simulated results compared with the SeaWiFS measurements for the wavelengths of 443 and 670 nm and for various cases: (a) & (b) the Rayleigh atmosphere, (c) & (d) the two-layer SSA with aerosols located at the bottom 2-km layer (mixed with 22% of molecules), and (e) & (f) the two-layer SSA with water cloud located at the bottom 2-km layer (mixed with 22% of molecules).

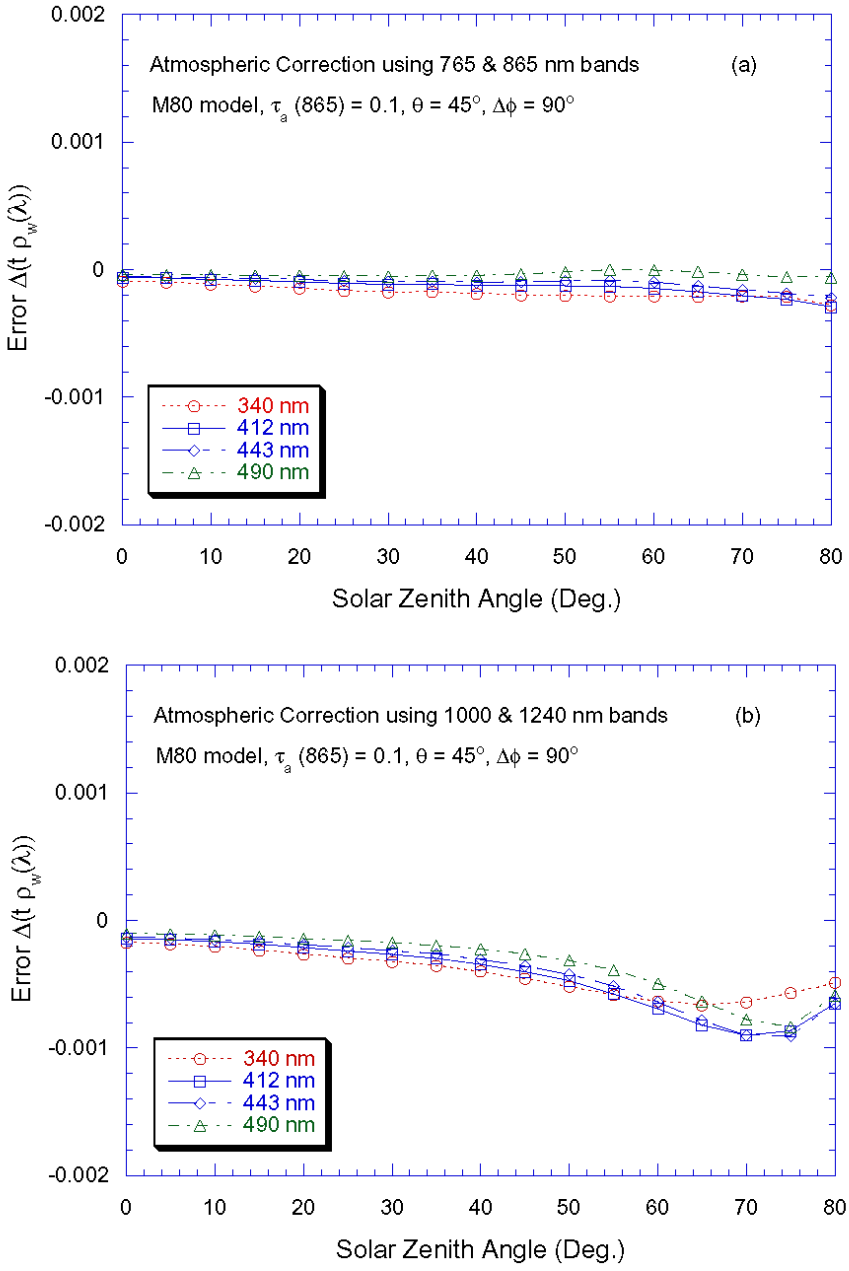

Figure 19.2: Errors in the derived water-leaving reflectance with atmospheric correction using the NIR bands of (a) 765 and 865 nm and (b) 1000 and 1240 nm.

Atmospheric Correction using the Longer NIR Bands

For the Case-2 waters, the ocean is usually not black at the near-infrared (NIR) wavelengths centered at 765 and 865 nm, which are used for the atmospheric correction for both SeaWiFS and MODIS to derive the ocean color products (Gordon and Wang, 1994). In these cases, the ocean contributions at the NIR are often mistakenly accounted as radiance scattering from atmosphere, thereby leading to over-correction of atmospheric radiance and underestimation of water-leaving radiance at the visible. Simulations have been carried out for the atmospheric correction using the longer NIR bands centered at 1000, 1240, and 1640 nm for retrievals of the ocean color product in the coastal waters. At the longer NIR bands, ocean is black even for the Case-2 waters. Thus, the Case-2 bio-optical model that has strongly regional dependence is not needed for the atmospheric correction. The atmospheric correction can be therefore operated routinely for the global coastal waters, and the water-leaving radiance spectrum from blue to the short NIR in the coastal regions can be derived. This scheme can also be applied to the cases of Case-1 waters with high chlorophyll concentrations in which the ocean contributions at the short NIR bands (765 and 865 nm) are significant. The performance of the atmospheric correction using the longer NIR bands is compared with that of the SeaWiFS and MODIS algorithm using the 765 and 865 nm bands. Figure 19.3 provides examples of comparison results with the longer NIR for the atmospheric correction. Fig. 19.3 (a) is results of error in the derived water-leaving reflectance using the NIR bands of 765 and 865 nm, while Fig. 19.3 (b) is results of atmospheric correction using the longer NIR bands of 1000 and 1240 nm. In both cases, the errors are all within ~0.001 for the derived water-leaving reflectance for wavelengths from UV to the blue.

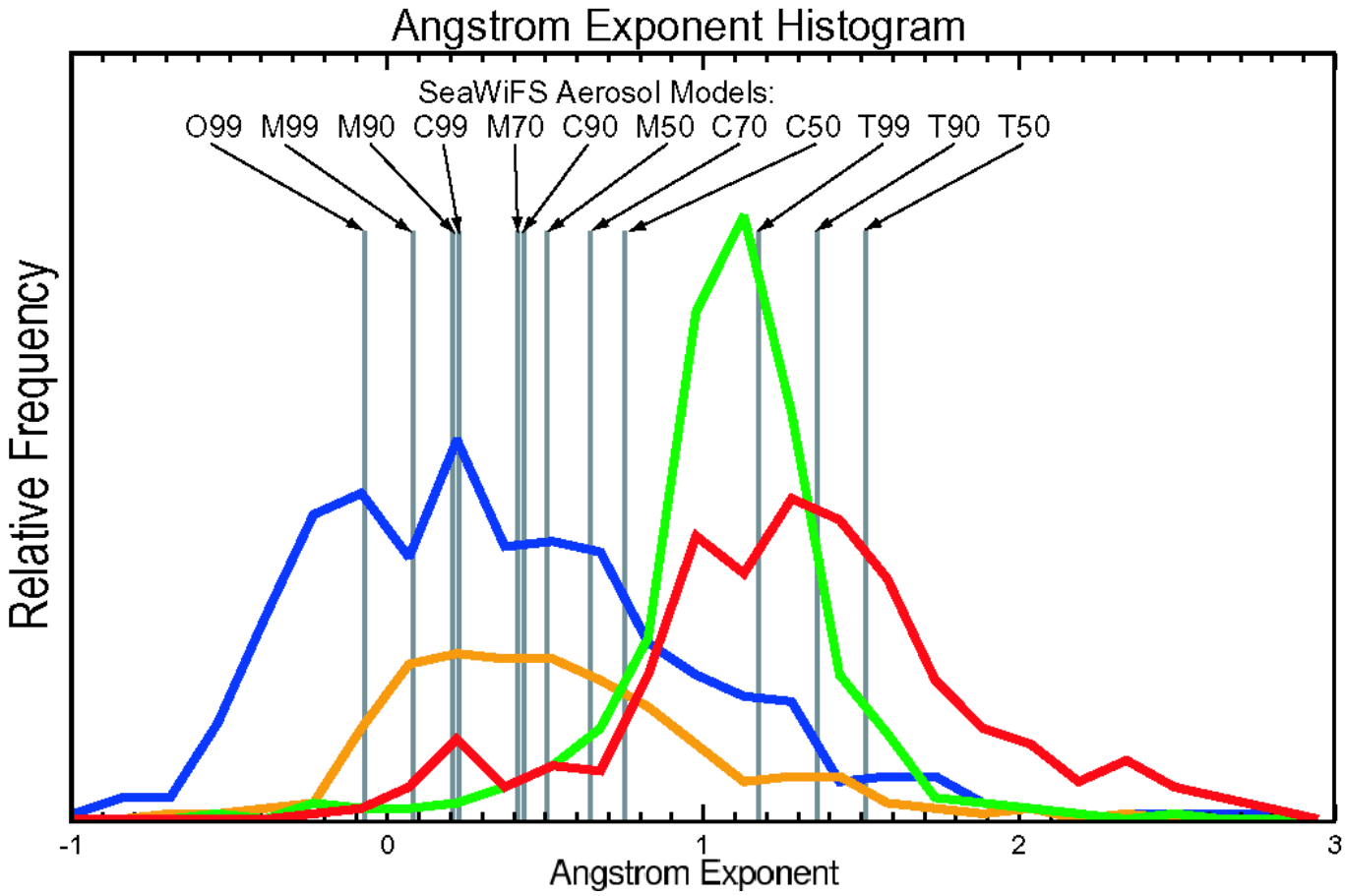

Figure 19.3: The Ångström exponents from the SeaWiFS 12 aerosol models compared with the in situ data collected bye the NASA SIMBIOS project.

Aerosol Model Validation

This is part of work reported in Knobelspiesse et al. (2003), and complete descriptions and results analyses can be found in this paper. Here is brief description of the SeaWiFS aerosol models compared with the in situ measurements.

One of the main purposes for the NASA SIMBIOS in situ aerosol data collection over oceans is to compare and validate aerosol products derived from the ocean color sensors (Wang et al., 2000), in particular, to validate the aerosol models used for the data processing in deriving the ocean color products. The primary goals of the SeaWiFS mission are routine global ocean color measurements and ocean bio-optical property data. In retrieving the ocean near-surface signals from sensor-measured radiances at the satellite, however, the atmospheric and surface effects must be removed. This is known as *atmospheric correction* (Gordon and Wang, 1994) which removes more than 90% of the sensor-observed radiance in the visible spectrum. The SeaWiFS atmospheric correction algorithm (Gordon and Wang, 1994) uses two near-infrared (NIR) bands to estimate the aerosol optical properties and extrapolate these into the visible spectrum where the ocean color products are derived. In this process, aerosol models are needed.

The SeaWiFS 12 aerosol models are the Oceanic model with the relative humidity (RH) of 99% (O99), the Maritime model with RH of 50%, 70%, 90%, and 99% (M50, M70, M90, and M99), the Coastal model with RH of 50%, 70%, 90%, and 99% (C50, C70, C90, and C99), and the Tropospheric model with RH of 50%, 90%, and 99% (T50, T90, and T99) (Wang, 2000). The Oceanic, Maritime, and Tropospheic aerosol models are from (Shettle and Fenn, 1979), while the Coastal model was introduced by (Gordon and Wang, 1994). These aerosol models are all non- and weakly absorbing. Table 19.1 summarizes optical properties for these aerosol models. In Table 19.1, the Ångström exponent is the mean value for a given aerosol model, while the single-scattering albedo is value at the wavelength 865 nm. The same atmospheric correction algorithm with similar aerosol model set is used for the retrieval of the ocean color products from the Moderate Resolution Imaging Spectroradiometer (MODIS) (Esaias et al., 1998; Salomonson et al., 1989).

The aerosol model is defined by its particle size distribution and refractive indices (real and imaginary parts). The Ångström exponent is related to the particle size distribution. Low value of the Ångström exponent indicates the large particle size, while high value of the Ångström exponent represents the small particle size of aerosols. For a given aerosol particle size distribution (aerosol model), the Ångström exponent is defined. Therefore, the Ångström exponent values obtained from the ground in situ measurements can be used to indicate if an appropriate aerosol model set in terms of the particle size distribution is used for the SeaWiFS data processing. Note that, however, this only gives part of picture, i.e., the aerosol particle size distribution. To validate the aerosol model and give a complete picture, the refractive indices are also needed. The refractive indices (or aerosol single-scattering albedo) can be derived with the sky radiance measurements (Dubovik and King, 2000; Wang and Gordon, 1993).

Figure 19.3 provides comparison results of the Ångström exponent from the SeaWiFS 12 aerosol models with those of the in situ measurements. The Ångström exponent values for the SeaWiFS 12 aerosol models are represented as vertical lines which are compared with the histograms from all in situ data collected by the NASA SIMBIOS project (Knobelspiesse *et al.*, 2003). Clearly, the in situ Ångström exponents obtained from maritime environment can be well represented with the SeaWiFS 12 aerosol models in the most of time. It appeared that, however, in the open ocean regions aerosol models with much larger particle sizes (very small Ångström exponent values) may still needed, e.g., aerosol models reported by (Porter and Clarke, 1997). On the other hand, in the coastal regions, aerosol models with low values of the single-scattering albedo (absorbing aerosols), e.g., dust aerosol models, are needed to handle these absorbing aerosol cases (Moulin et al., 2001).

The IOCCG Atmospheric Correction Working Group Activity

I have been continuing on activities for the IOCCG atmospheric correction working group. The main objective of the working group is to quantify the performance of the various exiting atmospheric correction algorithms used for the various ocean color missions. Therefore, the derived ocean color products from various ocean color missions can be meaningfully compared and possibly merged.

Table 19.1. Characteristics of the 12 aerosol models for the SeaWiFS data processing.

Aerosol Model	Relative Humidity (%)	Symbol	Ångström Exponent	Single Scattering Albedo (865 nm)
Oceanic	99	O99	-0.086	1.0
Maritime	50, 70, 90, 99	M50-M99	0.091-0.502	0.981-0.999
Coastal	50, 70, 90, 99	C50-C99	0.224-0.757	0.971-0.997
Tropospheric	50, 90, 99	T50, T90, T99	1.185-1.519	0.930-0.987

REFERENCES

Ding, K., and H.R. Gordon, 1994: Atmospheric correction of ocean-color sensors: effects of the Earth's curvature, *Appl. Opt.*, **33**: 7096-7106.

Dubovik, O., and M. King, 2000: A flexible inversion algorithm for retrieval of aerosol optical properties from Sun and sky radiance measurements, *J. of Geophys. Res.*, **105**: 20,673-20696.

Esaias, W.E., M.R. Abbott, I. Barton, O.B. Brown, J.W. Campbell, K.L. Carder, D.K. Clark, R.L. Evans, F.E. Hodge, H.R. Gordon, W.P. Balch, R. Letelier, and P.J. Minnet, 1998: An overview of MODIS capabilities for ocean science observations, *IEEE Trans. Geosci. Remote Sens.*, **36**: 1250-1265.

Gordon, H.R., and M. Wang, 1994:, Retrieval of water-leaving radiance and aerosol optical thickness over the oceans with SeaWiFS: A preliminary algorithm, *Appl. Opt.*, **33:** 443-452.

Knobelspiesse, K.D., C. Pietras, G.S. Fargion, M. Wang, R. Frouin, M.A. Miller, A. Subramaniam, and W.M. Balch, 2003: Maritime aerosol optical properties measured by handheld sun photometers, *Remote Sens. Environ.* (Submitted).

Moulin, C., H.R. Gordon, R.M. Chomko, V.F. Banzon, and R.H. Evans, 2001: Atmospheric correction of ocean color imagery through thick layers of Saharan dust, *Geophys. Res. Letters*, **28:** 5-8.

Porter, J.N., and A.D. Clarke, 1997: Aerosol size distribution models based on in situ measurements, *J. of Geophys. Res.*, **102**: 6035-6045.

Salomonson, V.V., W.L. Barnes, P.W. Maymon, H.E. Montgomery, and H. Ostrow, 1989: MODIS: advanced facility instrument for studies of the Earth as a system, *IEEE Trans. Geosci. Remote Sensing*, **27**: 145-152.

Shettle, E.P., and R.W. Fenn, 1979: Models for the Aerosols of the Lower Atmosphere and the Effects of Humidity Variations on Their Optical Properties, *AFGL-TR-79-0214*, , U.S. Air Force Geophysics Laboratory, Hanscom Air Force Base, Mass.

Wang, M., 2000: The SeaWiFS atmospheric correction algorithm updates, Vol. **9**, *NASA Tech. Memo. 2000-206892*, S.B. Hooker and E.R. Firestone, Eds., SeaWiFS Postlaunch Technical Report Series, NASA Goddard Space Flight Center, Greenbelt, Maryland.

Wang, M., 2003: Light scattering from spherical-shell atmosphere: Earth curvature effects measured by SeaWiFS, *Eos, Transactions, American Geophysical Union* (In press).

Wang, M., S. Bailey, and C.R. McClain, 2000: SeaWiFS Provides Unique Global Aerosol Optical Property Data, in *Eos, Transactions, American Geophysical Union*, pp. 197.

Wang, M., and H.R. Gordon, 1993: Retrieval of the columnar aerosol phase function and single scattering albedo from sky radiance over the ocean: simulations, *Appl. Opt.*, **32**: 4598-4609.

This Research was Supported by
the NASA Contract # 00203

Publications

Wang, M., 1999: Validation study of the SeaWiFS oxygen A-band absorption correction: Comparing the retrieved cloud optical thicknesses from SeaWiFS measurements, *Appl. Opt*., **38**, 937-944.

Wang, M., 1999: Atmospheric correction of ocean color sensors: Computing atmospheric diffuse transmittance, *Appl. Opt*. , **38**, 451-455.

Wang, M., 1999: A sensitivity study of SeaWiFS atmospheric correction algorithm: effects of spectral band variations*, Remote Sens. Environ*., **67,** 348-359.

Siegel, D. A., M. Wang, S. Maritorena, and W. Robinson, 2000: Atmospheric correction of satellite ocean color imagery: the black pixel assumption, A*ppl. Opt*., **39**, 3582-3591.

Eplee, R. E., Jr., W. D. Robinson, S. W. Bailey, D. K. Clark, P. J. Werdell, M. Wang, R. A. Barnes, and C.R. McClain, 2001: The calibration of SeaWiFS, Part 2: Vicarious techniques, *Appl. Opt.,* **40**, 6701-6718.

Wang, M. and S. W. Bailey, 2001: Correction of the sun glint contamination on the SeaWiFS ocean and atmosphere products, *Appl. Opt.,* **40**, 4790-4798.

Wang, M., B. A. Franz, R. A. Barnes, and C. R. McClain, 2001: Effects of spectral bandpass on SeaWiFS-retrieved near-surface optical properties of the ocean, *Appl. Opt*., **39**, 343-348.

Chou, M. D., P. K. Chan, and M. Wang, 2002: Aerosol radiative forcing derived from SeaWiFS-retrieved aerosol optical properties, *J. Atmos. Sci.,* **59**, 748-757.

Gregg, W. W., M. E. Conkright, J. E. O'Reilly, F. S. Patt, M. Wang, J. Yoder, and N. Casey-McCabe, 2002: NOAA-NASA Coastal Zone Color Scanner reanalysis effort, *Appl. Opt***., 41**, 1615-1628.

Wang, M. and H. R. Gordon, 2002: Calibration of ocean color scanners: How much error is acceptable in the near-infrared, *Remote Sens. Environ***., 82**, 497-504.

Wang, M., 2002: The Rayleigh lookup tables for the SeaWiFS data processing: Accounting for the effects of ocean surface roughness, *Int. J. Remote Sens.,* **23**, 2693-2702.

Wang, M., 2003: An efficient method for multiple radiative transfer computations and the lookup table generation, *J. Quant. Spectr. Rad. Trans*., **78**, 471-480.

Wang, M., 2003: Correction of artifacts in the SeaWiFS atmospheric correction: Removing the discontinuity in the derived products, *Remote Sens. Environ*., **84**, 603-611, 2003.

Tanaka, T. and M. Wang, 2003: Solution of radiative transfer in anisotropic plane-parallel atmosphere*, J. Quant. Spectr. Rad. Trans*. (In press).

Wang, M., Extrapolation of the aerosol reflectance from the near-infrared to the visible: the single-scattering epsilon vs. multiple-scattering epsilon method, *Int. J. Remote Sens*. (In press).

Wang, M., Light Scattering from Spherical-Shell Atmosphere: Earth curvature effects measured by SeaWiFS, *Eos, Transaction, American Geophysical Union*, (In press).

Other publications

Wang, M., 1998: Applying the SeaWiFS atmospheric correction algorithm to MOS: Effects of spectral band variations, Proc. the 4th Pacific Ocean Remote Sensing Conference, p88-91, Qingdao, China, July 28-31.

Wang, M., 1998: A validation of the SeaWiFS O2 A-band absorption correction, Proc. the 4th Pacific Ocean Remote Sensing Conference, p32-36, Qingdao, China, July 28-31.

Wang, M. and B. A. Franz, 1998: A vicarious intercalibration between MOS and SeaWiFS, Proc. 2nd International Workshop on MOS-IRS and Ocean Colour, p95-102, Berlin, Germany, June 10-12.

Wang, M., S. W. Bailey, C. R. McClain, C. Pietras, and T. Riley, 1999: Remote sensing of the aerosol optical thickness from SeaWiFS in comparison with the in situ measurements, Proc. Ocean color, land surface, radiation and clouds, aerosols: the contribution of new generation spaceborne sensors to global change studies, Méribel, France, WK1-O-08, p1-4, January 18-22.

Wang, M., 2000: Effects of the sea surface wind speed on the SeaWiFS derived ocean color optical property data, Proc. the ONR's Ocean Optics XV [CD-ROM], Musée Océanographique, Monaco, October 16-20.

Wang, M. and S. W. Bailey, 2000: Correction of the sun glint contamination, Proc. the 5th Pacific Ocean Remote Sensing Conference, p18-22, Goa, India, December 5-8.

Liberti, G. L, F. D'Ortenzio, R. Santoleri, G. L. Volpe, M. Wang, C. R. McClain, and V. E. Cachorro Revilla, 2001: Validation of SeaWiFS aerosol products over the Mediterranean basin," Proc. EUMETSAT Meteorological Satellite Data Users' Conference, p18-22, Antaya, Turkey, October 1-5.

Wang, M., 2002: Approaches of the aerosol correction algorithm: methods of the single-scattering vs. multiple-scattering epsilon," Proc. the ONR's Ocean Optics XVI [CD-ROM], Santa Fe, New Mexico, November 18-22.

Wang, M., 2002: Example of aerosol model effects in SeaWiFS atmospheric correction," Proc. SPIE's Third International Asia-Pacific Symposium on Remote Sensing of the Atmosphere, Ocean, Environment, and Space, Vol. 4892, p87-94, Hangzhou, China, October 23-27.

Presentations

Chou, M. D., P. K. Chan, and M. Wang, 1999: Global aerosol radiative forcing derived from SeaWiFS-inferred aerosol optical properties, The AGU Fall Meeting, San Francisco, California, December 13-17.

Wang, M. and S. W. Bailey, 2000: Correction of the sun glint contamination," The 5th Pacific Ocean Remote Sensing Conference, Goa, India, December 5-8.

Wang, M., 2000: Effects of the sea surface wind speed on the SeaWiFS derived ocean color optical property data," The Ocean Optics XV, Musée Océanographique, Monaco, October 16-20.

Wang, M., 2000: Effects of the vicarious calibration on the SeaWiFS derived aerosol optical properties, The AGU Spring Meeting, Washington, DC, May 30-June 3.

Wang, M., A. Isaacman, B. A. Franz, and C. R. McClain, 2001: A comparison study of the ocean color data derived from OCTS and POLDER, The AGU Fall Meeting, San Francisco, California, December 10-14, 2001.

Gales, J. M., B. A. Franz, and M. Wang, 2001: A three year intercomparison of oceanic optical properties from MOS and SeaWiFS, The AGU Fall Meeting, San Francisco, California, December 10-14.

Wang, M., 2002: Examples of the aerosol model effects in the SeaWiFS atmospheric correction," SPIE's Third International Asia-Pacific Symposium on Remote Sensing of the Atmosphere, Ocean, Environment, and Space, Hangzhou, China, October 23-27.

Wang, M., 2002: Approaches of the aerosol correction algorithm: Methods of the single-scattering vs. multiple-scattering epsilon," The Ocean Optics XVI, Santa Fe, New Mexico, November 18-22.